Third International Symposium on Marine Propulsors
smp'13, Launceston, Tasmania, Australia, May 2013

Uncertainty in Bollard Pull Predictions

Arthur Vrijdag[1], Jochem de Jong[1], Hain van Nuland[2]

[1]Damen Shipyards Research Department, Gorinchem, the Netherlands
[2]MSc-student Marine Technology, Technical University Delft, the Netherlands

ABSTRACT

An important aspect for a new-built tug is the contracted bollard pull performance. Not reaching the contracted bollard pull can lead to penalties for the shipbuilder and dissatisfaction for the customer while an under predicted bollard pull can lead to non-competitive design and a lower income for the shipbuilder. The bollard pull performance of a new-built tug is uncertain due to the uncertainties that are involved in the design and building of the tug and in its propulsion installation. Furthermore uncertainty is introduced during the full scale trial measurements at which the bollard pull is to be demonstrated. This paper aims at the quantification of the uncertainties that are involved in the bollard pull performance prediction. This is done by systematic analysis of the propagation of uncertainty from input (design) variables up to the predicted bollard pull performance.

Keywords

Bollard pull, uncertainty analysis, sensitivity, prediction

1 INTRODUCTION

As said, the most important performance indicator of a tug is its maximum bollard pull. It is therefore important that the prediction of bollard pull receives considerable attention during the various stages of design.

When a tug is sold, a specific bollard pull value is to be agreed upon by the shipbuilder and the customer, which is subsequently formalised in the sales contract. Based on the shipbuilders experience a certain margin is applied to the calculated theoretical bollard pull prediction. The size of this correction is traditionally based on experience and is in fact a balance between risk and reward: a high contract value may lead to high reward (profit for the shipbuilder), but may also easily lead to a penalty and dissatisfaction if the contracted bollard pull is not met.

During the sea trials the vessel performance in terms of manoeuvrability, ship speed and also bollard pull is measured by means of specialised equipment (see Figure 1). In case of the bollard pull test, a certified load cell is to be used.

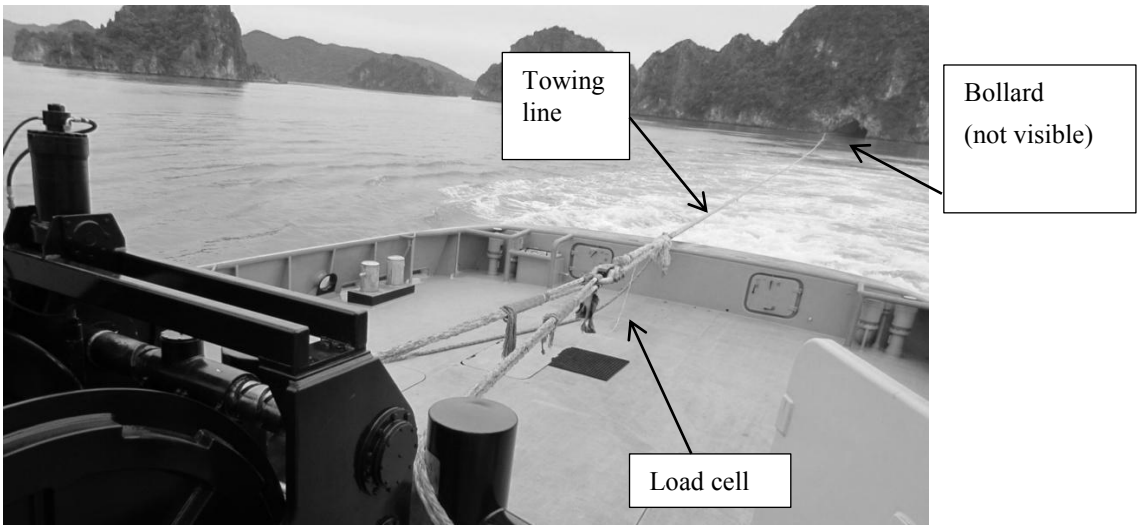

Figure 1: Execution of a bollard pull test. Wireless load cell readout panel not visible

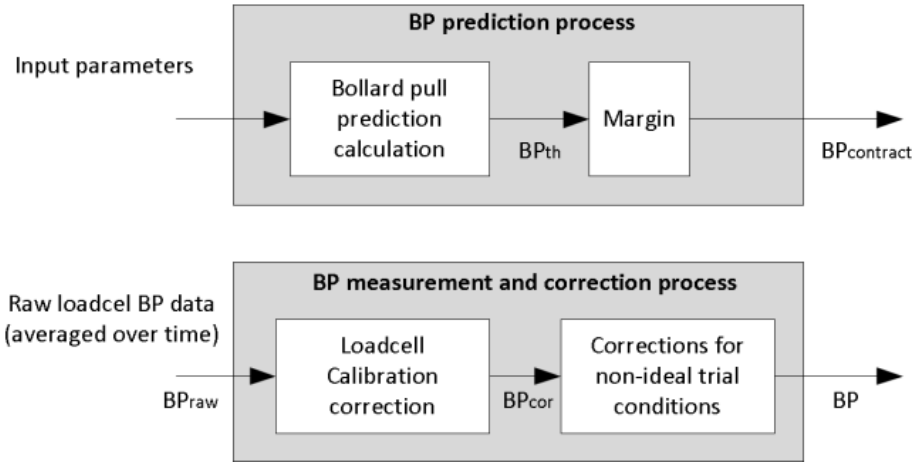

Figure 2: Bollard pull prediction and bollard pull measurement and correction.

.

The measured values are corrected according to the load cell calibration table as given by the certification authority. If required, further corrections are applied to take into account non-ideal trial conditions such as for instance limited towing cable length and limited water depth. Examples of such correction methods are for instance given by Jukola and Skogman (2002). The corrected bollard pull value represents the bollard pull value in ideal trial conditions, and should meet the bollard pull value as stated in the contract.

In this paper the uncertainties that are involved in the prediction and measurement of the bollard pull value are put in a framework. This is done by means of grouping the various contributors to the uncertain prediction on the one hand and by grouping the contributors to the uncertain measurement and the uncertain trial conditions on the other hand.

The focus in this paper lies on quantification of the uncertainty in the bollard pull prediction due to uncertainty in the parameters that are used to calculate the BP prediction.

2 TYPES OF UNCERTAINTY

As explained by Schulten and Stapersma (2007), various types of uncertainty can be identified such as:

- Theory uncertainty
- Model uncertainty
- Parametric / variable uncertainty
- Measurement uncertainty

Theory uncertainty is the uncertainty in the underlying physical principles of the model. Examples of underlying physical principles are the laws of Newton, which are not uncertain at all if the model deals with classical mechanics. Models regarding quantum mechanics can however be assumed to have some degree of uncertainty in the underlying physical principles.

Model uncertainty is a direct result of the fact that a model is a simplified representation of reality. In Schulten and Stapersma (2007) a further subdivision is made, but this is outside the scope of this paper. Estimation of model uncertainty is in theory possible by comparing outcomes of models of various levels of complexity. Since a model often consists out of many sub models and underlying assumptions this soon becomes a practically impossible option.

Parametric / variable uncertainty indicates the uncertainty which is introduced due to uncertainty in the parameters and input variables of the model under consideration. Typical examples are the gravitational acceleration, the density of water, the diameter of the propeller and so on.

Measurement uncertainty is the uncertainty introduced in the measurement and processing phase.

3 EFFECT OF UNCERTAINTY ON BOLLARD PULL

How these various types of uncertainty play a role in the prediction and measurement of the bollard pull performance of a ship is illustrated in Figure 2.

On the upper left hand side the input parameters to the bollard pull prediction calculation process are shown as starting point. Because some input parameters are not 100% certain, this introduces parameter uncertainty. The prediction model itself is based on well-established physical principles so no theory uncertainty is assumed to play a role. The model itself is however a simplified representation of reality and therefore this does result in model uncertainty. The size of this model uncertainty is however hard to estimate.

Subsequently a specific margin is applied which results in the contract value which is to be met. No uncertainty is added in this step.

On the bottom left hand side the uncorrected load-cell measurement readouts (averaged over a considerable length of time) are used as input. Subsequently the load

cell calibration corrections are applied to obtain the corrected bollard pull in non-ideal trial conditions. Clearly measurement uncertainty is introduced here.

If the effect of non-ideal trial conditions is significant, further corrections can be applied. This is done by calculating the effect of these non-ideal conditions by making use of "correction models", which introduce additional uncertainty (examples are: correction for limited water depth, limited towing line length, current or wind). On the one hand this can be seen as introduction of additional model and parameter uncertainty. On the other hand this can be seen as measurement uncertainty because it is part of the "measurement and correction process". Although this is a matter of choice, the latter is assumed here.

The end result of the bottom block diagram is the measured bollard pull value corrected to ideal conditions. This value should meet the contract BP value.

In this paper the focus lies on estimation of the effect of parameter uncertainty that is introduced in the "bollard pull prediction process". In the next section a method to estimate output uncertainty is introduced in a general way. Subsequently the bollard pull prediction method is explained, and finally a case study is used to demonstrate the application of the method to a specific case. The same method has been applied to ship speed predictions in Vrijdag and de Vos (2012).

4 QUANTIFICATION OF UNCERTAINTIES

The output uncertainty can be quantified by determining the output sensitivity and input uncertainty and then combining these two:

Output sensitivity: In terms of the block diagram shown in Figure 3, the output sensitivities are expressed as $\frac{\partial z}{\partial x}$, which are often presented as the normalised sensitivities $\frac{\partial z^*}{\partial x} = \frac{\partial z}{\partial x} \cdot \frac{x_0}{z_0}$, where x_0 and z_0 are the nominal values of input and output. This normalised presentation allows for a more intuitive interpretation, since it expresses the percentage of change in output based on a percentage change in input.

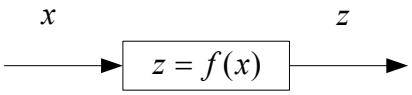

Figure 3: General block diagram with input x and output z.

Input uncertainty: The uncertainty in input variables can be quantified in various ways. Mostly a Gaussian (normal) distribution is assumed, which can be defined via its mean value μ_x and its standard deviation σ_x. Other often-used ways of expressing the size of uncertainty are the variance σ_x^2 and the 95% interval, which roughly is the interval described by $[\mu_x - 2\sigma_x, \mu_x + 2\sigma_x]$. It can be convenient to use the normalised uncertainty $\sigma_x^* = \frac{\sigma_x}{\mu_x}$.

Output uncertainty can now be determined by combining output sensitivities and input uncertainties via

$$\sigma_z^2 = \sum_i \left(\frac{\partial z}{\partial x_i} \right)^2 \cdot \sigma_{x_i}^2 \quad \text{.....(1)}$$

the output uncertainties are obtained. This equation holds under the assumption that the input parameters x_i are mutually independent.

If the previously introduced normalised sensitivities and uncertainties are used, this equation changes to:

$$\left(\sigma_z^*\right)^2 = \sum_i \left(\frac{\partial z}{\partial x_i}^* \right)^2 \cdot \left(\sigma_{x_i}^*\right)^2 \quad \text{.....(2)}$$

Another possible method to obtain the output uncertainties is via Monte Carlo Simulation (MCS). The principle of MCS is to calculate the output variables over and over again, while randomly picking the input values from their (not necessarily Gaussian) distributions. If this calculation is carried out enough times, the output distribution will be found. This method is however not used here since, although perhaps giving a more accurate numerical answer, it does not provide direct insight into the variables that play the biggest role during uncertainty propagation. In particular MCS does capture non-linear effects in the underlying mathematical model, while usage of $\frac{\partial z}{\partial x}$ implicitly assumes a linear system so that theoretically the method is only exact for infinitesimal input uncertainties. By systematic investigation it has however been concluded that the ship propulsion system under consideration behaves closely to linear for reasonably sized variations of input parameters.

The assumption of a Gaussian distribution of the various uncertain input parameters might not always hold if very detailed information on the actual distribution would be available. However, such detailed data is practically not available and estimation of non-Gaussian distributions seems difficult, even for subject matter experts.

5 BOLLARD PULL PREDICTION METHOD

Before the theory as explained above is applied in a case study, the bollard pull prediction method is explained. As the most important commercial contract value is the bollard pull, the needed power is estimated by empirical specific thrust figures. A specific engine is selected in order to reach this bollard pull value. In order to keep propeller blade load and propeller blade tip speed within reasonable limits, propeller diameter and gearbox ratio are dictated. Often this is done based on experience and fine-tuned in further design iterations. In order to make use of the full engine brake power P_B for the bollard pull, it is ensured in the design strategy that the bollard pull propeller line intersects in the upper right hand corner of the engine envelope. (see Figure 4 for an example)

The available brake power P_B is delivered to the propeller via shaft and gearbox, resulting in the propeller power P_p according to:

$$P_p = P_B \cdot k_e \cdot \eta_{trm} \quad \text{.....(3)}$$

where k_e is the number of engines per shaft and η_{trm} is the transmission efficiency which contains both the shaft efficiency and the gearbox efficiency:

$$\eta_{trm} = \eta_s \cdot \eta_{gb} \quad \text{.....(4)}$$

The open water propeller power P_o is related to the propeller power P_p via the relative rotative efficiency η_R:

$$P_o = \eta_R \cdot P_P \quad \text{.....(5)}$$

The open water propeller torque Q in the upper right hand corner of the engine envelope is defined by:

$$Q_{design} = \frac{P_o}{2\pi n_{p,\max}} \quad \text{.....(6)}$$

where $n_{p,\max}$ is the maximum propeller speed, related to the maximum engine speed at maximum power.
From here the design propeller torque coefficient $K_{Q,design}$ can be calculated:

$$K_{Q,design} = \frac{Q_{design}}{\rho n_{p,\max}^2 D^5} \quad \text{.....(7)}$$

A design towing speed $v_{s,design}$ needs to be chosen now, which in most textbooks is chosen as 0 kts. Dependent on the application higher values can be selected as well. The selected design towing speed in combination with the wake fraction w and the maximum propeller speed $n_{p,\max}$, delivers the design advance ratio J_{design}, which in this case equals zero:

$$J_{design} = \frac{v_{s,design} \cdot (1-w)}{n_{p,\max} D} \quad \text{.....(8)}$$

The design advance ratio, in combination with the design torque coefficient $K_{Q,design}$ and systematic propeller series data (such as for instance the Wageningen Ka-19A series) fixes the $\left(P/D\right)_{design}$ value and the resulting design thrust coefficient $K_{T,design}$ of the propeller.
The bollard pull prediction (for a range of engine speeds) can now be done as follows: Based on the $\left(P/D\right)_{design}$ value that has been determined above, the propeller thrust T and torque Q values are calculated by making use of:

$$T = K_T \cdot \rho \cdot n_p^2 \cdot D^4$$
$$Q = K_Q \cdot \rho \cdot n_p^2 \cdot D^5 \quad \text{.....(9)}$$

The open water propeller torque curve can be transformed to the brake power curve by:

$$P_B = \frac{2\pi \cdot n_p \cdot Q}{k_e \cdot \eta_R \cdot \eta_{trm}} \quad \text{.....(10)}$$

The Pb-n-BP relation is visualised in Figure 4 and Figure 5.

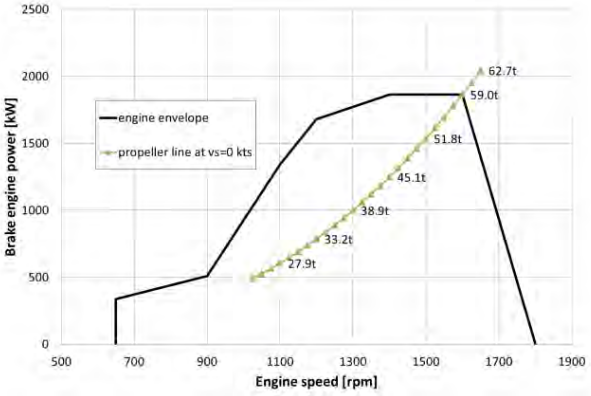

Figure 4: Predicted propeller operating line in ideal bollard pull conditions.

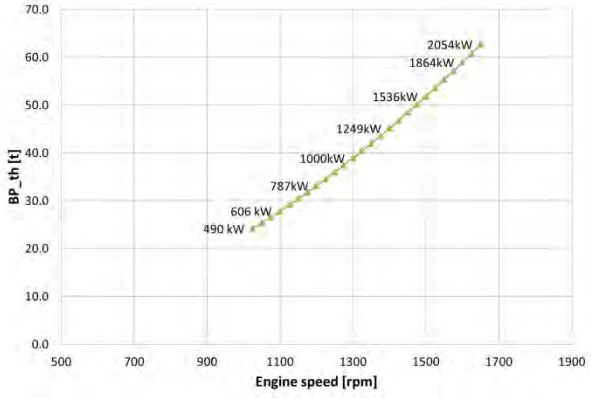

Figure 5: Predicted relation between bollard pull and rpm.

To obtain the theoretically (maximum) achievable bollard pull value (BP_{th}) in [tons] the thrust is corrected for thrust deduction $(1-t)$ and divided by the gravitational acceleration g:

$$BP_{th} = \frac{k_p \cdot T \cdot (1-t)}{1000 \cdot g} \quad \text{.....(11)}$$

where k_p is the number of driving propellers. This bollard pull value is the theoretically achievable bollard pull in ideal conditions without any margin. Often a margin X is applied in the following way to arrive at the BP value that is to be stated in the contract:

$$BP_{contract} = BP \cdot (1-X) \quad \text{.....(12)}$$

This margin X is traditionally based on experience with other vessels. In the following section a more scientific approach to the determination of sensible margin values is discussed.

6 CASE STUDY

To demonstrate the use of the uncertainty analysis technique a case study is performed here.

The imaginary ship under consideration is a twin shaft tug with two 1865bkW, 1600rpm high-speed diesel engines, two gearboxes and two 2.4m CPPs in nozzles.

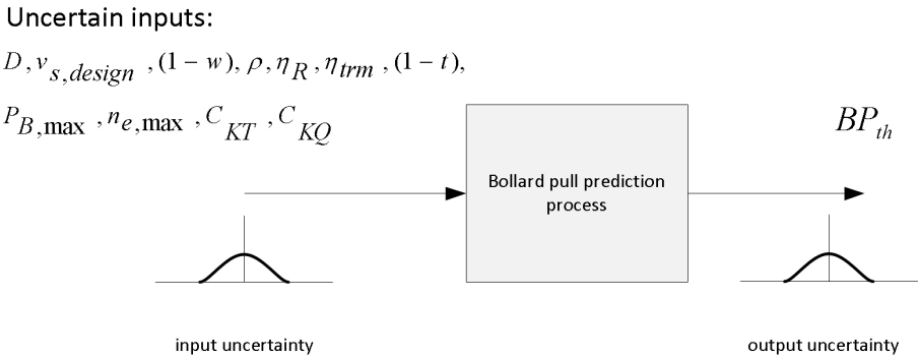

Figure 6: Uncertain inputs of the bollard pull prediction.

The theoretical bollard pull value is predicted based on nominal values of various uncertain inputs which are shown in Figure 6. Note that there is some room for debate in the selection of uncertain input parameters. One could for instance argue that the expanded blade area ratio EAR is uncertain during design because one simply cannot exactly know what EAR will be selected by the propeller manufacturer. On the other hand one can argue that this uncertainty does not need to be incorporated explicitly, but can implicitly be taken into account by assuming uncertainty in the open water propeller polynomials that are used. This uncertainty in OW polynomials will include uncertainties in EAR, pitch distribution, and other aspects. This will take into account the uncertain differences between the propellers and nozzles that are used during design (for instance Wageningen Ka-19a open water data) and the propeller and nozzle as will be installed in the real world. In this paper it is chosen to lump the propeller related uncertainties together in two parameters: C_{K_Q} and C_{K_T}. These input parameters are used to "model" uncertainty in open water curves in the following way:

$$K_Q = C_{K_Q} \cdot K_{Q,polynomial} \quad \text{.....(13)}$$

The nominal value of these two parameters is 1.

As described above the squared uncertainties in outputs z are defined by:

$$\left(\sigma_z^*\right)^2 = \sum_i \left(\frac{\partial z}{\partial x_i}^* \right)^2 \cdot \left(\sigma_{x_i}^*\right)^2 \quad \text{.....(14)}$$

The **sensitivities** $\frac{\partial z^*}{\partial x_i}$ are determined first. This is done by running the analysis several times, while one-by-one applying small perturbations to the uncertain input parameters, while at the same time retaining the design point. Outputs that are presented here are BP_{th} (Figure 7), and propeller pitch P/D (Figure 8).

The sensitivities of BP_{th} should be interpreted as follows: *The effect of a +1% variation in* η_R *is a +0.7% variation in* BP_{th}. *This includes the effect of* P/D *adjustment.*

It can also be seen that the highest sensitivities are related to thrust deduction and the K_T correction factor. If the real K_Q value turns out to be 1% higher than assumed, this will lead to a 0.4% reduction of P/D, and a bollard pull reduction of 0.7%.

Sensitivities of other propulsion related variables have been determined as well, but are not presented here. Only their final output uncertainties are presented later on.

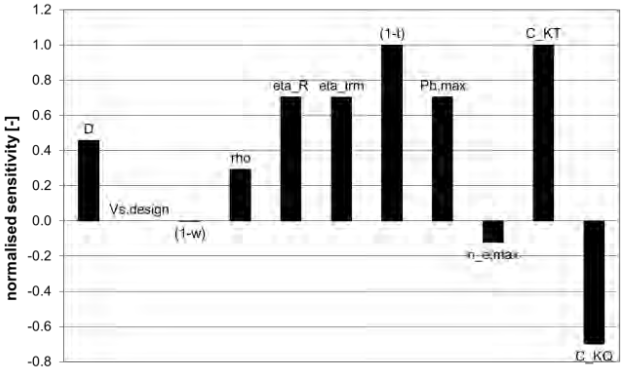

Figure 7: Normalised sensitivities of BP_{th} to various input parameters.

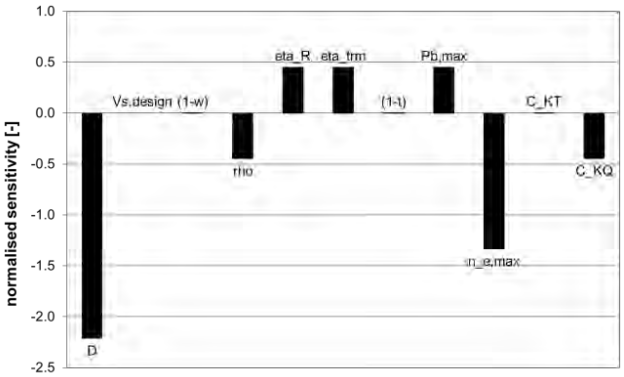

Figure 8: Normalised sensitivities of P/D to various input parameters.

Next, the normalised **input uncertainties** $\sigma_{x_i}^*$ are to be selected. Ideally uncertainty values would be based upon empirical data. Unfortunately such data is hard to come by and if existent it remains to be seen whether equipment manufacturers and model basins are always willing to share such data.

In Longo and Stern (2005) an example is given on how to derive uncertainty values of data resulting from model tests. Mentioned approach is tailored towards sailing at forward speed. A similar approach can probably be taken for bollard pull measurements at zero speed. Some of the uncertain model test data (such as t and w) can be used as input for further theoretical work and the size of its uncertainty is therefore relevant.

For this case study no model test data is available and therefore nominal values of the various inputs are based on experience with similar vessels. Input uncertainties are estimated by means of expert opinion, based on experience and spread of data known/ derived from other similar projects. The assumption is that the first of class of ships is considered and that no "learning effect" has taken place yet by making use of full scale measurement data of sister- vessels.

Although not ideal, the assumption is that results based on expert opinion will at least result in increased understanding and a good indication of uncertainty.

The assumed input uncertainties are shown in Figure 9. The figure for instance shows that the assumed uncertainty in transmission efficiency $\sigma^*_{\eta_{trm}}$ is 2%, which is equivalent to stating that the 95% confidence interval of η_{trm} is $\left[\mu_{\eta_{trm}} \pm 4\%\right]$.

Greatest uncertainty is assumed in (1-w), and least uncertainty is assumed in the seawater density and the propeller diameter.

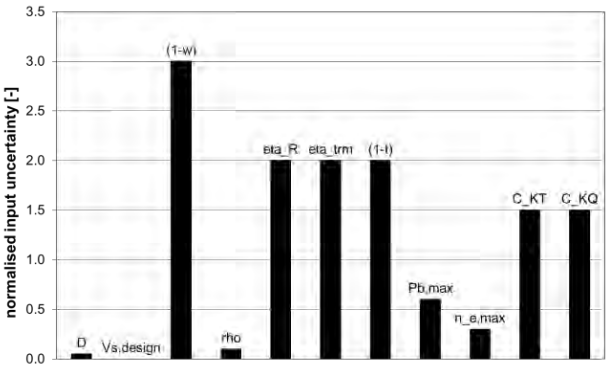

Figure 9: Normalised input uncertainties, based on expert opinion.

Combination of sensitivity and uncertainty results in an estimated output uncertainty as shown in Figure 10, where besides BP_{th} and P/D other variables are shown as well. As shown the uncertainty in BP_{th} is 3.4%, while the uncertainty in P/D is 1.5%.

This means that for a predicted theoretical bollard pull of 59 ton, the 95% confidence interval is given by $\left[55.0 - 63.0\right]$ton, as visualised in Figure 11.

If only parameter uncertainty is assumed, and no measurement uncertainty is taken into account, based on Figure 11 there is an 80% chance that a bollard pull of >57.3 ton is realised. There is only a 20% likelihood that >60.7 ton will be realised. The BP that is to be stated in the contract can now be selected based on a trade-off between risk and reward for the shipbuilder and the customer. This example shows that the discussed uncertainty analysis method can be used to support determination of sensible bollard pull contract values.

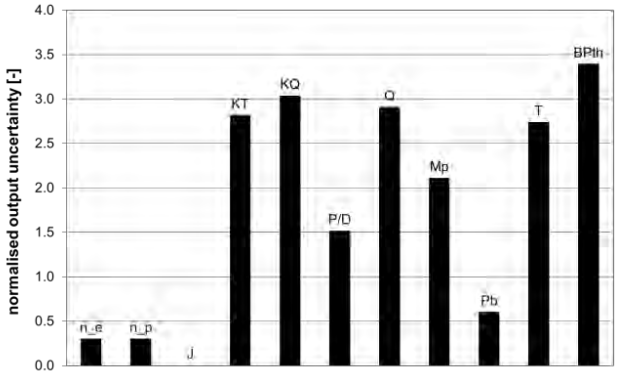

Figure 10: Normalised output uncertainty of various output variables.

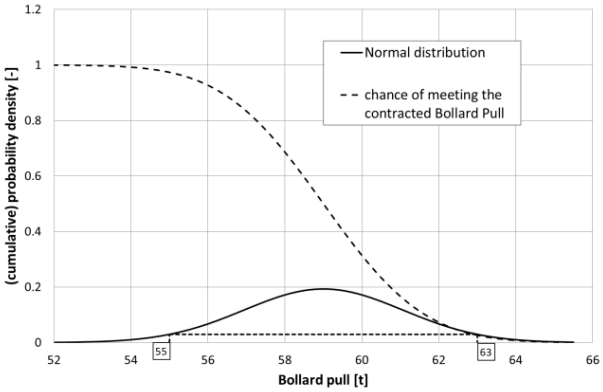

Figure 11: (cumulative) probability density function.

The case study as was performed here involved a CPP ship. It was assumed that the CPP is adjusted during the BP trial to make the propeller line intersect the upper right hand corner of the engine envelope. This adjustment is however not possible for FPPs, which results in two possible cases: the real propeller line intersects the envelope at maximum rpm, or the propeller line intersects the envelope at max power. This introduces a non-linearity, which is not captured correctly by the uncertainty analysis method as used here. Monte Carlo simulation would however allow for output uncertainty estimation of such a "highly non-linear system".

7 CONCLUSIONS AND RECOMMENDATIONS

In this paper the uncertainties that are involved in bollard pull predictions and measurements were put in a framework. Subsequently an uncertainty analysis method was introduced and applied to a bollard pull prediction.

The quantification of the uncertainties in input parameters remains a difficult issue, and therefore expert opinion is used in this paper.

Despite the crude method of input parameter uncertainty estimation, the uncertainty analysis as carried out here gives some indication of the size of deviations that are to be expected between the real bollard pull and the predicted bollard pull.

Better insight and understanding of the importance of uncertainty analysis will likely lead to more attention for the determination/ estimation of these input uncertainties.
Another important in-between result of the uncertainty analysis as carried out here are the graphs showing the sensitivities. These graphs help to identify those parameters that require most attention during the design process.
Ultimately the proposed approach can help to determine sensible margin values and resulting contract bollard pull values, instead of making use of a rule-of-thumb margin factor that is based on previous experience. This is especially attractive in case of first of class ships for which no full scale reference data is available.
To allow for uncertainty analysis of (ship propulsion) systems that include strong non-linearities, it is recommended to investigate the merits of Monte-Carlo simulation.

For various reasons the Bollard Pull prediction process as used by the Damen Research Department at some points deviates from the approach as described in this paper. This mainly has to do with the "learning effect" that takes place by repeatedly building and commissioning vessels of the same type.

ACRONYMS

CPP	Controllable Pitch Propeller
EAR	Expanded Area Ratio
FPP	Fixed Pitch Propeller
MCS	Monte Carlo Simulation
OW data	Open water propeller data

REFERENCES

Joe Longo and Fred Stern (2005), „Uncertainty Assessment for Towing Tank Tests With Example for Surface Combatant DTMB Model 5415". Journal of Ship Research, Vol 49, No 1, pp 55-68.

Hanna Jukola and Anders Skogman (2002), „Bollard Pull". Proceedings of the 17th International Tug & Salvage convention and exhibition. Bilbao, Spain, pp 189-197.

Schulten, P., and Stapersma, D. (2007). „A study of the validity of a complex simulation model". Journal of Marine Engineering and Technology No. AI0. pp. 67-77.

Vrijdag, A and de Vos, P. (2012). „Uncertainties and margins in the ship propulsion system design process." Proceedings of the 11th International Naval Engineering Conference (INEC), Edinburg, UK. pp 618-630.

NOMENCLATURE

BP	Bollard pull
D	Propeller diameter
g	Gravitational acceleration
i	Gearbox ratio
J	Advance ratio
k_e	Number of engines per shaft
k_p	Number of propellers
K_Q	Torque coefficient
K_T	Thrust coefficient
M_p	Propeller torque
n_e	Engine speed
n_p	Propeller speed
P_B	Brake power
P_D	Total Propeller power
P_e	Effective power
P_p	Propeller power
P_{PTO}	PTO power
P/D	Pitch ratio
Q	Open water propeller torque
R	Resistance
t	Thrust deduction factor
T	Thrust
th	Theoretical
v_a	Advance speed
v_s	Ship speed
w	Wake factor
X	Margin on bollard pull
x	Input parameter
z	Immersion of propeller/ output variable
η_0	Open water propeller efficiency
η_{trm}	Transmission efficiency
η_R	Relative rotative efficiency
ρ	Seawater density
σ_x	Standard deviation of variable x
μ_x	Mean value of variable x